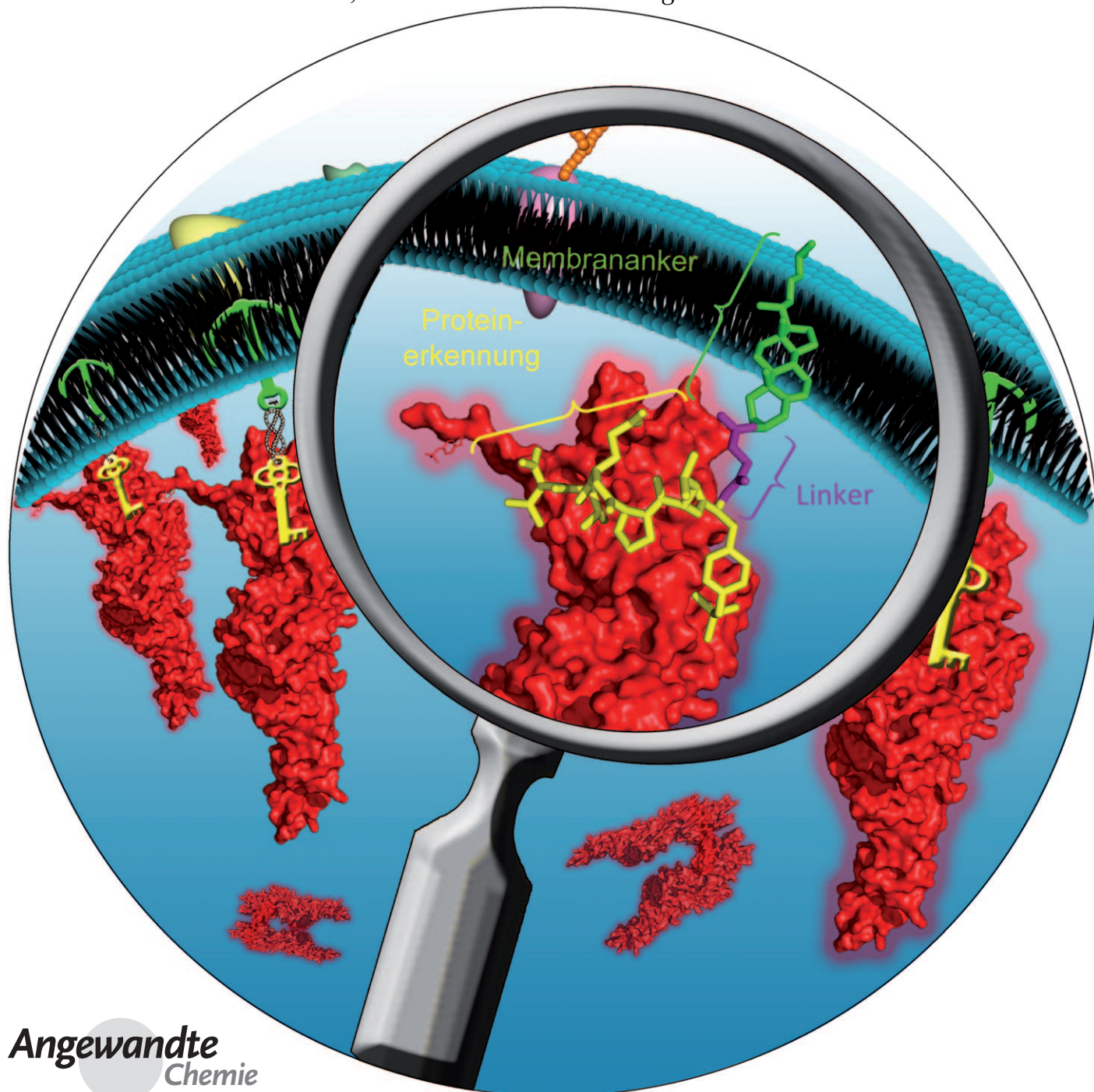


# Artificially Induced Protein–Membrane Anchorage with Cholesterol-Based Recognition Agents as a New Therapeutic Concept\*\*

Miriam Avadisman, Steven Fletcher, Baoxu Liu, Wei Zhao, Peibin Yue, Daniel Badali, Wei Xu, Aaron D. Schimmer, James Turkson, Claudiu C. Gradinaru,\* and Patrick T. Gunning\*



Angewandte  
Chemie

Nature has developed a vast array of post-translational modifications that result in physical changes in protein characteristics, functionality, and cellular location. An ingenious cellular mechanism for protein localization is prenylation: the covalent attachment of a hydrophobic prenyl group to a protein to facilitate protein association with the plasma membrane.<sup>[1]</sup> Analogous post-translational modifications that induce protein–membrane anchorage include the covalent attachment of glycolipid anchors (glycosylphosphatidylinositol, GPI)<sup>[2]</sup> and palmitoyl groups.<sup>[3]</sup> Through these processes, otherwise soluble proteins are sequestered to cellular membranes and ultimately lose their cellular motility.<sup>[4]</sup>

We postulated that the induced membrane anchorage of proteins involved in cancer-promoting cell-signaling cascades could hold significant therapeutic value. Thus, we wished to explore the therapeutic potential of applying the principles of protein anchorage to the development of a conceptually novel drug modality. Our objective was to develop a scaffold that could effectively restrict the motility of a cancer-promoting protein within a cellular environment (Figure 1) and thereby inhibit its function. Herein, we demonstrate the in vitro application of this inhibition strategy and show the first example of induced protein–membrane anchorage through the use of a rationally designed protein–membrane anchor (PMA).

To demonstrate this principle, we chose to target the oncogenic signal transducer and activator of transcription 3 (STAT3) protein, a master regulator of the underlying events in malignant transformation. Conceptually, our approach represents a departure from traditional inhibitors of STAT3 cell-signaling pathways. Previous strategies have focused primarily on the suppression of upstream kinases<sup>[5]</sup> and STAT3–STAT3 protein–protein interactions.<sup>[6]</sup> To date, these approaches have not yielded a clinically relevant STAT3-targeting drug. STAT3 plays a key role in relaying cytokine or growth-factor signaling to the nucleus, where it binds to specific DNA-response elements in the promoters of target genes and thereby induces cancer-promoting gene-expression profiles. Thus, our goal was to develop an inhibitor

that could sequester STAT3, a 93 kDa protein, at the plasma membrane and suppress nuclear translocation through PMA-induced protein–membrane association.

Herein, we describe the design, synthesis, and application of a novel PMA that targets STAT3 protein in liposome and whole-cell systems. The prototype PMA was composed of two binding modules: a recognition motif to bind the protein (STAT3) and an anchor to sequester the protein complex at the membrane. Proof-of-concept PMA **1** (Figure 1) comprised a potent STAT3-recognition sequence GpYLPQTV-NH<sub>2</sub><sup>[7]</sup> covalently attached to a cholesterol membrane anchor through the N terminus. The GpYLPQTV-NH<sub>2</sub> peptide sequence binds to the Src homology 2 (SH2) domain of STAT3. It is the most potent STAT3 binder that has been described and is an excellent handle for the coupling of our lipid anchors.<sup>[6a]</sup> Owing to facile synthetic procedures and potent membrane insertion, we elected to employ cholesterol as our membrane anchor in preference to prenyl and GPI lipids. Moreover, in support of this strategy, Simons and co-workers have successfully used cholesterol to anchor drugs that target membrane-embedded proteins to the plasma membrane.<sup>[8]</sup> We attached the peptide to the cholesterol unit in high yield through chloroformate coupling (see the Supporting Information). Furthermore, to examine the role played by the linking group, we prepared a PMA in which an extended poly(ethylene glycol) linker (PEG) was used to link the peptide and cholesterol moieties (PMA **2**; Figure 1). As a control compound, we synthesized a bivalent fluoresceinated probe, **3**, which incorporates a 5-aminofluorescein moiety between the cholesterol unit and the peptide (Figure 1).

To evaluate whether the ditopic inhibitor **1** conserved its STAT3-binding capability when conjugated to the cholesterol steroid, we conducted control binding experiments with full-length STAT3 protein. The binding affinity of **1** was measured in a competitive fluorescence polarization (FP) assay popularly used to determine the affinity of the STAT3 SH2 domain for small molecules.<sup>[9]</sup> Encouragingly, we found that the cholesterol conjugate retained good binding potency for the STAT3 SH2 domain ( $K_i = 0.95 \pm 0.1 \mu\text{M}$ ; GpYLPQTV-NH<sub>2</sub>:  $K_i = 0.2 \mu\text{M}$ ).

To assess the efficacy of our STAT3 PMAs, we developed a series of in vitro fluorescence-based experiments to visualize PMA-induced STAT3 protein localization in lipid model systems. As part of these experiments, the cysteine thiol groups in the protein were labeled with tetramethylrhodamine, and the resulting protein (TMR–STAT3) was characterized by single-molecule spectroscopy (see the Supporting Information).<sup>[10]</sup> To assess whether fluorescence labeling compromised the phosphopeptide-binding function of the STAT3 SH2 domain, we conducted control experiments on a multiparameter confocal microscope.<sup>[11]</sup> Simultaneously detected polarization and fluorescence correlation data confirmed that the binding affinity of TMR–STAT3 for the inhibitor was similar to that of the unlabeled protein.<sup>[10]</sup> We conducted in vitro liposome experiments to determine whether PMAs could sequester a fluorescently labeled 93 kDa STAT3 protein at a lipid membrane. The experiments were monitored with custom-built fluorescence microscopes capable of the hyperspectral detection of single emitters.<sup>[11]</sup>

[\*] M. Avadisman,<sup>[‡]</sup> Dr. S. Fletcher,<sup>[‡]</sup> B. Liu,<sup>[‡]</sup> D. Badali, Prof. Dr. C. C. Gradinaru, Prof. Dr. P. T. Gunning  
Department of Chemical and Physical Sciences  
University of Toronto Mississauga  
Mississauga, ON L5L 1C6 (Canada)  
Fax: (+1) 905-828-5425  
E-mail: claudiu.gradinaru@utoronto.ca  
patrick.gunning@utoronto.ca

Dr. W. Zhao,<sup>[‡]</sup> Dr. P. Yue, Prof. Dr. J. Turkson  
Burnett School of Biomedical Sciences, College of Medicine  
University of Central Florida (USA)

Dr. W. Xu, Dr. A. D. Schimmer  
Ontario Cancer Institute/Princess Margaret Hospital (Canada)

[†] These authors contributed equally.

[\*\*] Financial support was provided by the Leukemia and Lymphoma Society of Canada (P.T.G., C.C.G., and J.T.), the NSERC (P.T.G., C.C.G.), the University of Toronto, a CIHR training award (B.L.), and NIH grants CA106439 and CA128865 (P.T.G. and J.T.).



Supporting information for this article is available on the WWW under <http://dx.doi.org/10.1002/anie.201102486>.

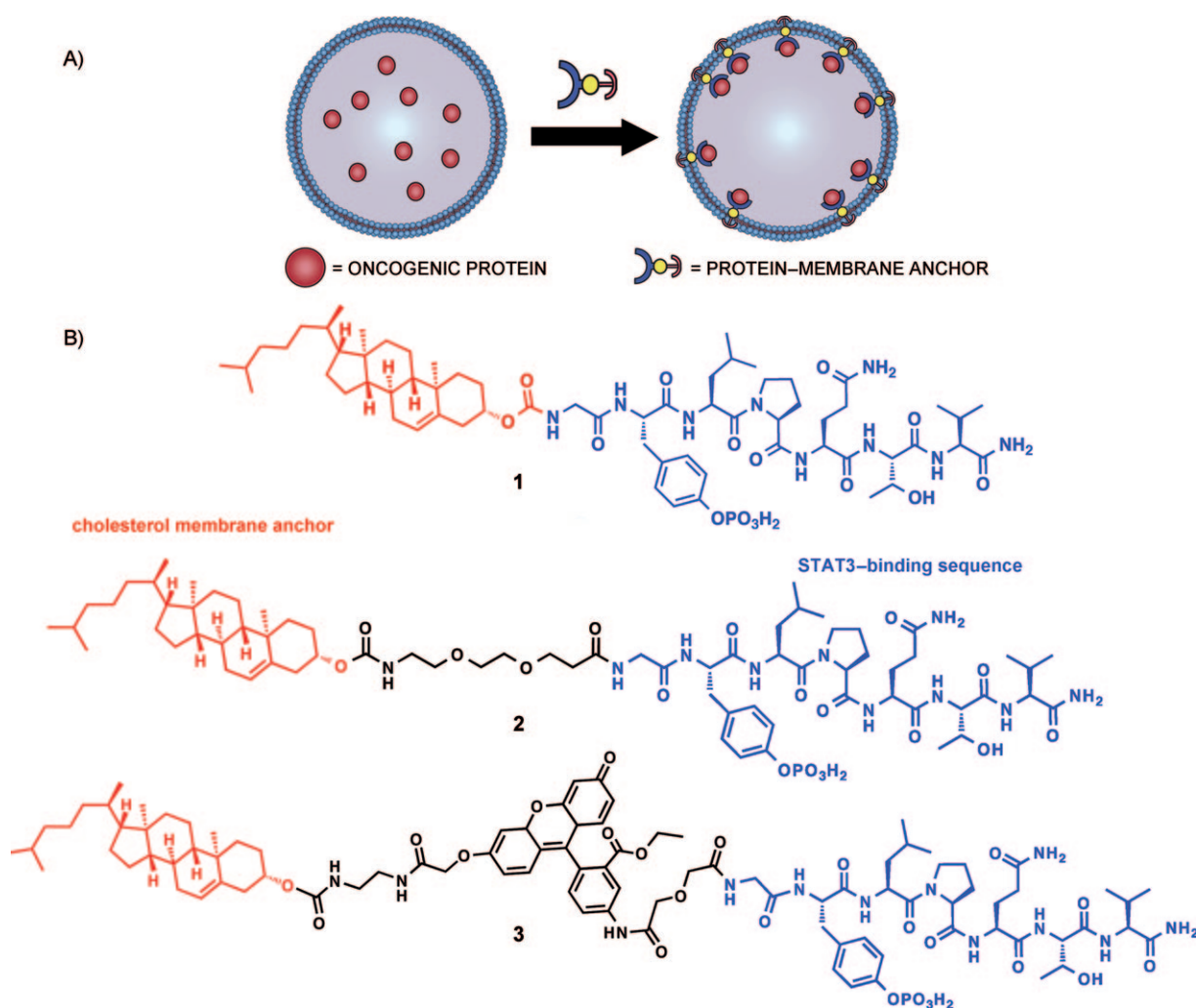


**Figure 1.** A) Strategy of protein-membrane anchorage. B) Chemical structures of PMAs **1**, **2**, and **3**.

Multilamellar vesicles (MLVs) and large unilamellar vesicles (LUVs) were prepared by using 1-palmitoyl-2-oleoyl-*sn*-glycero-3-phosphocholine (POPC) and biotinylated 1,2-bis-(dimethylphosphanyl)ethane (DMPE) by a previously reported extrusion protocol and tethered to a glass surface through a biotin-streptavidin linkage.<sup>[12]</sup>

In initial control experiments in which the distribution of the fluoresceinated PMA **3** in micrometer-sized lipid vesicles was imaged in the absence of STAT3 protein, we observed the unambiguous localization of **3** to the liposome boundary (Figure 2 A). As a further control, we prepared lipid vesicles

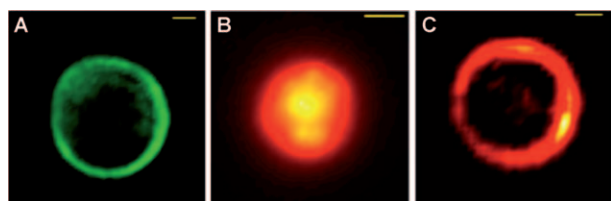


**Figure 2.** Wide-field fluorescence images of liposomes: A) an MLV prepared with PMA **3** (1 mol%); B) an LUV encapsulating TMR-STAT3 in the absence of the inhibitor; C) an MLV encapsulating TMR-STAT3 in the presence of PMA **1**. Scale bars: 1  $\mu$ m.

containing TMR-STAT3 only; in this case, in the absence of a PMA, TMR-STAT3 was distributed uniformly throughout the aqueous interior of the liposome (Figure 2 B). Further experiments conducted at varying STAT3 concentrations consistently showed similar protein distributions and thus confirmed that nonspecific adsorption of the protein to the lipid membrane was negligible. Remarkably, when the liposomes were treated with the nonfluorescent PMA **1** (1 mol%), TMR-STAT3 was sequestered at the liposome membrane: most of the TMR fluorescence originated from the membrane region (Figure 2 C). This dramatic change in the spatial distribution of STAT3 can be interpreted in terms of the strong binding affinity between the protein and the ligand, which is effectively tethered to the membrane through the cholesterol moiety (Figure 2 A). Continuous imaging of the liposomes for several minutes showed that the association of the protein with the lipid membrane was stable and that the interaction with PMA **1** was strong.

The STAT3-PMA **1**-membrane interactions were measured quantitatively by incubating TMR-STAT3 (50  $\mu$ L, 4 nM) on a POPC lipid bilayer supported on a glass coverslip (see the Supporting Information). In the absence of PMA **1**, the nonspecific absorption of single TMR-STAT3 proteins to

the lipid bilayer was observed by total internal reflection fluorescence (TIRF) imaging (Figure 3A). However, the nonspecific adhesion of the protein to the lipid surface was limited to  $12.4 \pm 2.6$  molecules for an area of  $16 \times 16 \mu\text{m}^2$  and was thus similar to the protein adhesion observed for the hydrophilic surface of cleaned glass coverslips. In contrast, when the lipid bilayer was exposed to PMA **1** (1 mol %) prior to incubation with TMR-STAT3, more than 450 proteins were sequestered to a lipid-surface area of identical size (Figure 3C).

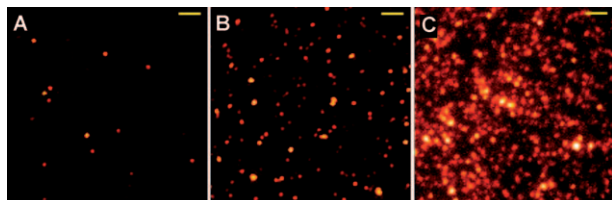


**Figure 3.** TIRF images of adsorbed TMR-STAT3 molecules on a supported lipid bilayer A) in the absence of **1**, B) in the presence of nonphosphorylated **1** (1 mol %), and C) in the presence of **1** (1 mol %). Scale bars: 2  $\mu\text{m}$ .

Since phosphopeptides are often dephosphorylated by intracellular phosphatases/esterases, we prepared a nonphosphorylated analogue of PMA **1** as a control to investigate whether phenolic species alone could sequester STAT3 at the lipid bilayer. Interestingly, the phenolic PMA elicited moderate levels of STAT3 membrane localization (Figure 3B) around four times higher than the nonspecific adsorption limit. This result was not unexpected, as both Dourlat et al. and our research group have reported a similar phenomenon, whereby the corresponding nonphosphorylated STAT3-binding sequence was found to retain moderate STAT3-binding activity.<sup>[13]</sup> The presence of the PEG linker in PMA **2** drastically reduced the membrane localization of STAT3 to about twice the level of the nonspecific adsorption limit (see the Supporting Information). This decrease in membrane localization may be caused by folding of the cholesterol-linker-peptide complex; folding of the complex could prevent both membrane anchoring and binding to STAT3.

In the case of PMA **1**, the surface coverage increased noticeably with incubation time and was limited only by the distribution of ligands on the surface of the bilayer. Successive imaging of the same membrane area showed that individual STAT3 molecules experienced lateral diffusion in the lipid membrane. Additional single-molecule spectroscopic experiments are currently under way to address in depth the dynamics of the ligand-protein interactions. Nevertheless, the preliminary biophysical data shown herein demonstrate unambiguously the potency of protein-specific PMAs.

The whole-cell inhibitory activity of PMA **1** was investigated in v-Src-transformed mouse fibroblasts, as previously described.<sup>[6]</sup> Briefly, NIH3T3/v-Src fibroblasts that harbor aberrant STAT3 activity were treated with **1** (at both 10 and 50  $\mu\text{M}$ ) for 24 h, and then nuclear extracts were prepared and subjected to a STAT3-STAT3:DNA-binding assay in vitro with an hSIE probe. The level of DNA-binding activity of

STAT3 protein was then determined by EMSA analysis (Figure 4A). Encouragingly, the potent STAT3-binding activity of PMA **1** in vitro was reflected in this assay, in which the DNA-binding activity of STAT3 was repressed significantly in a dose-dependent manner (Figure 4A). The reduced levels of STAT3 activity might indicate that PMA **1** anchors STAT3 to the membrane and thus prevents phosphorylation and subsequent nuclear translocation.

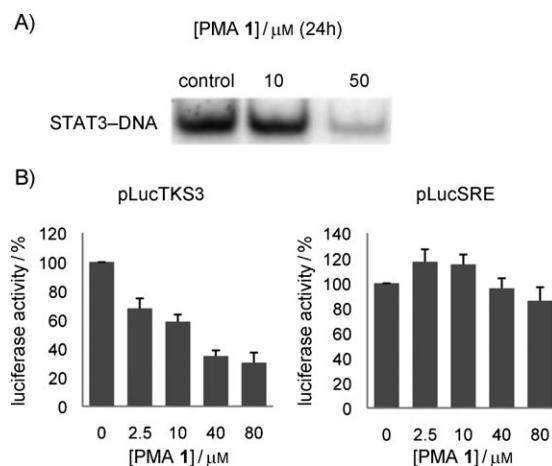


**Figure 4.** A) EMSA analysis of the inhibition of STAT3-STAT3 dimerization (as judged by the disruption of the STAT3-STAT3:DNA complex) by PMA **1** (10 and 50  $\mu\text{M}$ ) in whole NIH3T3/v-Src cells (the small-molecule inhibitor is absent in the control), as described previously.<sup>[6]</sup> The position of the STAT3-STAT3:DNA complex in the gel is shown; the results are representative of two independent assays. B) Cytosolic extracts of equal total protein were prepared from NIH3T3/v-Src fibroblasts (treated with PMA **1** for 24 h or untreated) that stably express the STAT3-dependent luciferase reporter (pLucTKS3) or from treated or untreated NIH3T3/v-Src fibroblasts that stably express the STAT3-independent luciferase pLucSRE and analyzed for luciferase activity with a luminometer.

Next, we conducted luciferase reporter studies to further determine the effects of **1** on the transcriptional activity of STAT3. Encouragingly, the results showed that the treatment of v-Src-transformed mouse fibroblasts (NIH3T3/v-Src), which stably express the STAT3-dependent luciferase reporter (NIH3T3/v-Src/pLucTKS3), with **1** at low-micromolar concentrations significantly repressed the induction of the STAT3-dependent reporter (Figure 4B). To examine nonspecific effects, we similarly treated NIH3T3/v-Src/pLucSRE fibroblasts, which overexpress the STAT3-independent luciferase reporter (pLucSRE), with **1** and performed a luciferase assay on the cytosolic extracts. Most encouragingly, STAT3-independent luciferase activity was not inhibited in cells treated with **1**, even at concentrations of up to 80  $\mu\text{M}$  (Figure 4B). These data corroborate the EMSA analysis of STAT3 DNA-binding activity and indicate that PMAs may specifically inhibit STAT3 nuclear translocation and thus inhibit the expression of genes targeted by STAT3.

To verify that PMAs inhibit STAT3 nuclear translocation, NIH3T3/hEGFR mouse fibroblasts overexpressing the human epidermal growth factor receptor (hEGFR) were starved of serum for 24 h and either treated or not with PMA

**1** for 3 h prior to stimulation with EGF for 15 min. Cells were then subjected to immunofluorescence staining for STAT3 (green) or staining of the nucleus with 2-(4-amidinophenyl)-1*H*-indole-6-carboxamide (DAPI) and analyzed by laser-scanning confocal microscopy for the inhibition of STAT3 nuclear translocation. In the resting NIH3T3/hEGFR fibroblasts, STAT3 (green) was predominantly distributed within the cytoplasm, with limited presence in the nucleus (blue; Figure 5 A–C). Subsequent stimulation of untreated cells with

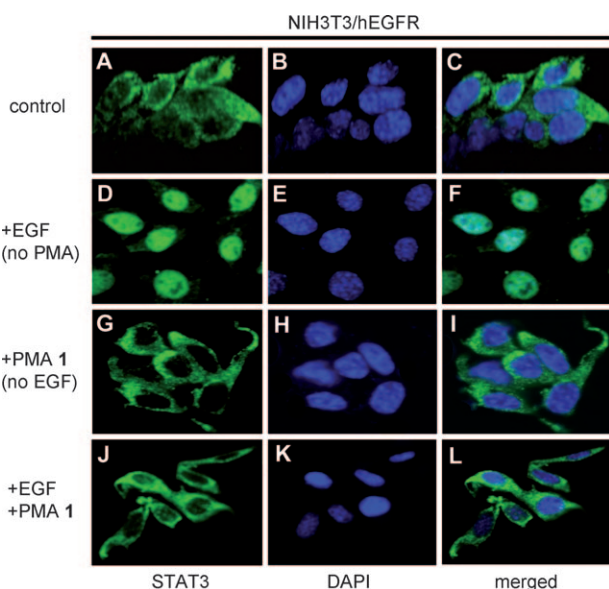


**Figure 5.** Inhibition of the EGF-induced nuclear translocation of STAT3 by PMA. Serum-starved NIH3T3/hEGFR cells were treated with PMA **1** (50  $\mu\text{M}$ ) for 3 h and then stimulated with recombinant human epidermal growth factor (rhEGF; 100 ng mL<sup>-1</sup>) for 15 min, immunostained with anti-STAT3 antibody (green) or stained with DAPI (nucleus, blue), and analyzed by laser-scanning confocal microscopy.

EGF induced a strong nuclear presence of STAT3 (cyan for merged STAT3 (green) and DAPI (blue-stained nucleus; Figure 5D–F). The treatment of resting NIH3T3/hEGFR cells with PMA **1** (50  $\mu\text{M}$ ) elicited a visible decrease in nuclear STAT3 protein and noticeable association with the cytoplasmic and intracellular membranes (Figure 5G–I). Most encouragingly, EGF-stimulated STAT3 nuclear localization was strongly blocked when cells were pretreated with PMA **1** (50  $\mu\text{M}$ ) before stimulation with EGF (Figure 5J–L), presumably through the PMA-mediated hindrance of the binding of the STAT3 SH2 domain to pTyr motifs of receptors and the prevention of de novo phosphorylation by tyrosine kinases. We conclude that PMA **1** probably captured STAT3 and anchored it to the membrane.

To further define the mode of action of the PMA and to confirm that the inhibitory effects observed are predominantly a consequence of the PMA-mediated localization of STAT3 exclusively to the plasma membrane, we conducted an immunofluorescence study in combination with laser-scanning confocal microscopy for the localization of STAT3. The human breast-cancer cell line MDA-MB-231, which harbors

constitutively active STAT3, was treated with PMA **1** (25  $\mu\text{M}$ ) and then subjected to staining with the plasma-membrane stain FM-4-64 (red) or the nuclear stain DAPI (blue), or to immunostaining with AlexaFluor488 antibody (green) for STAT3 detection. Again we observed complete inhibition of STAT3 nuclear translocation in PMA-treated cells, whereas in untreated MDA-MB-231 cells, activated STAT3 resided predominantly in the nucleus (Figure 6). Most encouragingly,

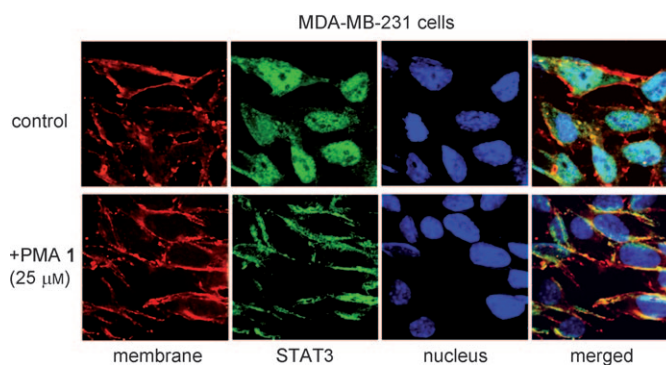


**Figure 6.** Induction of STAT3 membrane anchorage and inhibition of the nuclear translocation of STAT3 by PMA **1**. MDA-MB-231 breast-tumor cells were treated with PMA **1** (25  $\mu\text{M}$ ) for 6 h, immunostained with membrane stain FM-4-64 (red) or anti-STAT3 antibody (green) or stained with DAPI (nucleus, blue), and analyzed by laser-scanning confocal microscopy.

not only was STAT3 completely excluded from the nucleus in the presence of PMA **1**, but the colocalization images unequivocally showed that it was predominantly localized at the labeled plasma membrane (yellow). The present results provide a proof-of-concept for the membrane-anchoring properties of PMAs. Membrane anchorage is a novel mechanism for the inhibition of STAT3 function. Thus, prevention of the nuclear translocation of STAT3 inhibits its transcriptional function. As the probes contain a labile phosphotyrosine moiety, we recognize that biological activity may be decreased as a result of intracellular dephosphorylation and/or peptide hydrolysis. Thus, we are now in the process of preparing more metabolically resistant PMA inhibitors.

In summary, we have presented a novel inhibitor for the targeting of aberrant signaling proteins associated with human disease. We demonstrated that PMA-induced protein localization is a conceptually viable therapeutic strategy with STAT3 as our model in liposome, lipid-bilayer, and whole-cell systems. We envisage that the successful application of PMAs in tumors with aberrant STAT3 activity will be of significant therapeutic importance. Further studies to determine the biochemical and biological utility of more druglike, non-phosphorylated PMAs are ongoing. Future related approaches will incorporate more druglike, less peptidic STAT3 binders that are less prone to metabolic degradation.

Received: April 11, 2011

**Keywords:** antitumor agents · drug design · nuclear-translocation inhibitors · protein–membrane anchorage · protein–protein interactions

- 
- [1] R. Roskoski, Jr., *Biochem. Biophys. Res. Commun.* **2003**, *303*, 1–7.
- [2] D. Brown, G. L. Waneck, *J. Am. Soc. Nephrol.* **1992**, *2*, 895–906.
- [3] K. A. Cadwallader, H. Paterson, S. G. MacDonald, J. F. Hancock, *Mol. Cell. Biol.* **1994**, *14*, 4722–4730.
- [4] J. Güldenhaupt, Y. Adigüzel, J. Kuhlmann, H. Waldmann, C. Kötting, K. Gerwert, *FEBS J.* **2008**, *275*, 5910–5918.
- [5] J. De Vos, M. Jourdan, K. Tarte, C. Jasmin, B. Klein, *Br. J. Haematol.* **2000**, *109*, 823–828.
- [6] a) S. Fletcher, J. Turkson, P. T. Gunning, *ChemMedChem* **2008**, *3*, 1159–1168; b) S. Fletcher, J. A. Drewry, V. M. Shahani, B. D. G. Page, P. T. Gunning, *Biochem. Cell Biol.* **2009**, *87*, 825–833; c) X. Zhang, P. Yue, S. Fletcher, W. Zhao, B. D. G. Page, P. T. Gunning, J. Turkson, *Biochem. Pharmacol.* **2010**, *79*, 1398–1409; d) S. Fletcher, B. D. Page, X. Zhang, J. Singh, J. Turkson, P. T. Gunning, *ChemBioChem* **2009**, *10*, 1959–1964; e) P. K. Mandal, W. S. Liao, J. S. McMurray, *Org. Lett.* **2009**, *11*, 3394–3397; f) P. K. Mandal, D. Limbrick, D. R. Coleman, G. A. Dyer, Z. Ren, J. S. Birtwistle, C. Xiong, X. Chen, J. M. Briggs, J. M. McMurray, *J. Med. Chem.* **2009**, *52*, 2429–2442; g) B. D. G. Page, D. Ball, P. T. Gunning, *Expert Opin. Ther. Pat.* **2011**, *21*, 65–83; h) S. Haftchenary, M. Avadisian, P. T. Gunning, *Anti-Cancer Drugs* **2011**, *22*, 115–127.
- [7] Z. Ren, L. A. Cabell, T. S. Schaefer, J. S. McMurray, *Bioorg. Med. Chem. Lett.* **2003**, *13*, 633–636.
- [8] a) L. Rajendran, A. Schneider, G. Schlechtingen, S. Weidlich, J. Ries, T. Braxmeier, F. Schwille, J. B. Schulz, C. Schroeder, M. Simons, G. Jennings, H. J. Knoelker, K. Simons, *Science* **2008**, *320*, 520–523; b) L. Rajendran, H.-J. Knoelker, K. Simons, *Nat. Rev. Drug Discovery* **2010**, *9*, 29–42.
- [9] J. Schust, T. Berg, *Anal. Biochem.* **2004**, *330*, 114–118.
- [10] D. Badali, B. Liu, A. Mazouchi, M. Avadisian, P. T. Gunning, C. C. Gradinaru, *Univ. Toronto J. Undergrad. Life Sci.* **2010**, *4*, 18–23.
- [11] B. Liu, S. Fletcher, M. Avadisian, P. T. Gunning, C. Gradinaru, *J. Fluoresc.* **2009**, *19*, 915–920.
- [12] B. Liu, A. Mazouchi, C. C. Gradinaru, *J. Phys. Chem. B* **2010**, *114*, 15191–15198.
- [13] a) J. Doulat, W. Q. Liu, F. Sancier, T. Edmonds, P. Pamonsinlapatham, F. Cruzalegui, C. Garbay, *Biochimie* **2009**, *91*, 996–1002; b) V. M. Shahani, P. Yue, S. Fletcher, S. Sharmeen, M. A. Sukhai, D. P. Luu, X. Zhang, H. Sun, W. Zhao, A. D. Schimmer, J. Turkson, P. T. Gunning, *Bioorg. Med. Chem.* **2011**, *19*, 1823–1838.
-